Proc. 12th Int. Conf. on Hypernuclear and Strange Particle Physics (HYP2015)
JPS Conf. Proc. **17**, 051001 (2017)
https://doi.org/10.7566/JPSCP.17.051001

Baryon-baryon interaction from chiral effective field theory

Johann Haidenbauer

Institute for Advanced Simulation, Forschungszentrum Jülich GmbH, D-52428 Jülich, Germany

E-mail: j.haidenbauer@fz-juelich.de

(Received November 29, 2015)

Recent results from the ongoing study of the baryon-baryon interaction within chiral effective field theory (EFT) by the Jülich-Bonn-Munich Group are reported. Specifically, a calculation of the in-medium properties of a hyperon-nucleon (YN) interaction derived within chiral EFT and fitted to ΛN and ΣN scattering data is reviewed. Furthermore, the relevance of three-body forces for hypernuclei is addressed and potentials for the leading order three-baryon interactions are discussed, which involve contact terms and irreducible one- and two-meson exchange diagrams. Finally, first results for baryon-baryon scattering in the strangeness $S = -2$ sector, obtained in chiral EFT up to NLO, are presented.

KEYWORDS: chiral effective field theory, baryon-baryon interaction

1. Introduction

In the present paper selected results from studies of the baryon-baryon interaction within chiral effective field theory (EFT) by the Jülich-Bonn-Munich group are reported. Those investigations are based on the scheme proposed by Weinberg which has been applied rather successfully to the nucleon-nucleon interaction in the past [1, 2]. In that approach there is an underlying power counting which allows to improve calculations systematically by going to higher orders in a perturbative expansion. In addition, it is possible to derive two- and corresponding three-body forces as well as external current operators in a consistent way. The focus in the present overview is on baryon-baryon systems with strangeness $S = -1$ and -2, i.e. on ΛN and ΣN scattering, and on the $\Lambda\Lambda$ and ΞN interactions.

I start by briefly reviewing results for the ΛN and ΣN interactions in free space, obtained up to next-to-leading order (NLO) in the chiral expansion [3]. At that order there are contributions from one- and two-pseudoscalar-meson exchange diagrams and from four-baryon contact terms without and with two derivatives. SU(3) flavor symmetry is imposed for constructing the hyperon-nucleon (YN) interaction in order to reduce the number of free parameters, in particular the number of low-energy constants (LECs) associated with the arising contact terms. In the actual calculation the SU(3) symmetry is broken, however, by the mass differences between the involved mesons (π, K, η) and between the baryons (N, Λ, Σ). An excellent description of available ΛN and ΣN scattering data could be achieved at NLO [3].

Then results for the in-medium properties of this YN are presented [4,5]. In particular, the single-particle potentials for the Λ and Σ hyperons in nuclear matter are evaluated in a conventional G-matrix calculation, and the Scheerbaum factor [6] associated with the hyperon-nucleus spin-orbit interaction is computed. One issue of special interest is the Σ-nucleus potential. There is strong phenomenological evidence that it is repulsive [7]. However, phenomenological models of the YN interaction based on meson-exchange, fitted to ΛN and ΣN scattering data, often fail to produce a repulsive Σ-nuclear potential.

Another issue of interest is the Λ-nucleus spin-orbit interaction where empirical information

suggests that it should be rather weak [8–10]. Therefore, we investigated also the spin-orbit interaction and, in particular, the role of the antisymmetric spin-orbit force in the YN system [4]. As mentioned above, the chiral EFT approach yields a potential that contains, besides pseudoscalar meson exchanges, a series of contact interactions with an increasing number of derivatives. In this approach a contact term representing an antisymmetric spin-orbit force arises already at NLO. It induces ${}^1P_1$–${}^3P_1$ transitions in the coupled (isospin $I = 1/2$) ΛN–ΣN system. The low-energy constant associated with the contact term could not be pinned down by a fit to the existing ΛN and ΣN scattering data as found in Ref. [3] and, thus, it was simply put to zero in that work. However, its value can be fixed from investigating the properties of the Λ hyperon in nuclear matter and, specifically, it can be utilized to achieve a weak Λ-nuclear spin-orbit potential [4, 5].

Afterwards I turn to three-body forces. Recently, the leading order three-baryon potential has been derived consistently within SU(3) chiral EFT. It involves contact terms and irreducible one- and two-meson exchange diagrams [11].

Finally, first results for baryon-baryon systems with strangeness $S = -2$, obtained in chiral EFT up to NLO, are presented and discussed [12].

2. The YN and YY interactions in chiral EFT

The derivation of the chiral baryon-baryon potentials for the strangeness sector at leading order (LO) using the Weinberg power counting is outlined in Refs. [13, 14]. Details for the NLO case can be found in Ref. [3], see also [15]. The LO potential consists of four-baryon contact terms without derivatives and of one-pseudoscalar-meson exchanges while at NLO contact terms with two derivatives arise, together with contributions from (irreducible) two-pseudoscalar-meson exchanges. The contributions from pseudoscalar-meson exchanges (π, η, K) are completely fixed by the assumed SU(3) flavor symmetry. On the other hand, the strength parameters associated with the contact terms, the LECs, need to be determined in a fit to data. How this is done is described in detail in Refs. [3, 12]. Note that we impose also SU(3) symmetry constraints for those contact terms which reduces the number of independent LECs that can contribute.

The reaction amplitudes are obtained from the solution of a coupled-channels Lippmann-Schwinger (LS) equation for the derived interaction potentials:

$$T^{\rho''\rho',J}_{\nu''\nu'}(p'', p';\sqrt{s}) = V^{\rho''\rho',J}_{\nu''\nu'}(p'', p') + \sum_{\rho,\nu}\int_0^\infty \frac{dpp^2}{(2\pi)^3} V^{\rho''\rho,J}_{\nu''\nu}(p'', p)\frac{2\mu_\nu}{q_\nu^2 - p^2 + i\eta} T^{\rho\rho',J}_{\nu\nu',J}(p, p';\sqrt{s})\,. \quad (1)$$

The label ν indicates the particle channels and the label ρ the partial wave. μ_ν is the pertinent reduced mass. The on-shell momentum in the intermediate state, q_ν, is defined by $\sqrt{s} = \sqrt{m^2_{B_{1,\nu}} + q_\nu^2} + \sqrt{m^2_{B_{2,\nu}} + q_\nu^2}$. Relativistic kinematics is used for relating the laboratory momentum $p_{\rm lab}$ of the hyperons to the c.m. momentum.

We solve the LS equation in the particle basis, in order to incorporate the correct physical thresholds. Depending on the total charge, up to three baryon-baryon channels can couple in case of the $\Lambda N - \Sigma N$ system and up to six channels in case of $\Lambda\Lambda - \Xi N - \Sigma\Lambda - \Sigma\Sigma$. In the $S = -1$ sector there are data at energies close to the thresholds and, therefore, in this case the Coulomb interaction is taken into account appropriately via the Vincent-Phatak method [16]. However, we omit the Coulomb interaction in our $S = -2$ calculation where, at present, such a more elaborate treatment is not required. The potentials in the LS equation are cut off with a regulator function, $f_R(\Lambda) = \exp\left[-\left(p'^4 + p^4\right)/\Lambda^4\right]$, in order to remove high-energy components [17]. We consider cutoff values in the range $\Lambda = 550 - 700$ MeV (LO) and $\Lambda = 500 - 650$ MeV (NLO), similar to what was used for chiral NN potentials

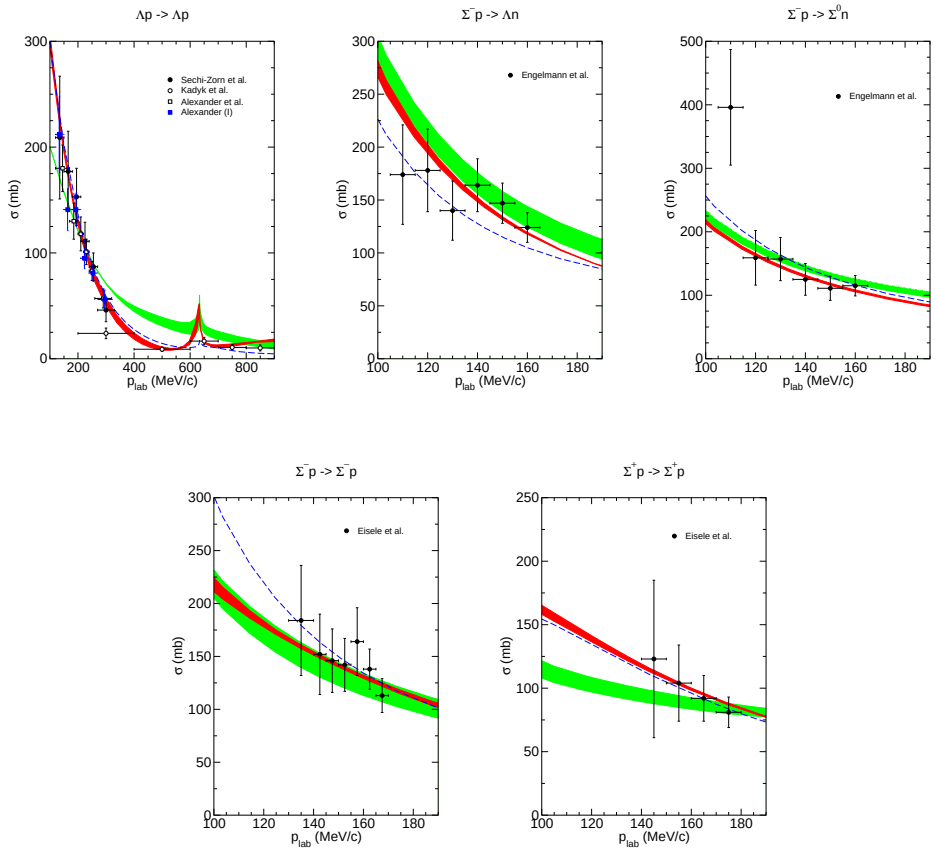

Fig. 1. Total cross sections for ΛN and ΣN scattering as a function of the laboratory momentum p_{lab}. The green/grey band shows the chiral EFT results to LO for variations of the cut-off in the range Λ = 550–700 MeV, while the red/black band are results to NLO for Λ = 500–650 MeV. The dashed curve is the result of the Jülich '04 [18] meson-exchange potential.

[17]. The cut-off dependence (represented by bands in the figures below) provides a lower limit of the theoretical uncertainty.

3. Results for ΛN and ΣN in free space

Our results for ΛN and ΣN scattering are presented in Fig. 1. The bands (red/black for NLO and green/grey for LO) represent the variation of the cross sections based on chiral EFT within the considered cutoff region, i.e. 550-700 MeV in the LO case [13] and 500-650 MeV at NLO. For comparison also results for the Jülich '04 [18] meson-exchange model are shown (dashed line).

Obviously, the available ΛN and ΣN scattering data are very well described by our NLO EFT interaction. In particular, and as expected, the energy dependence exhibited by the data is visibly better reproduced within our NLO calculation than at LO. This concerns especially the $\Sigma^+ p$ channel. But also for Λp the NLO results are now well in line with the data even up to the ΣN threshold. Furthermore, one can see that the dependence on the cutoff mass is strongly reduced in the NLO case. Additional results, for differential cross sections and for phase shifts, can be found in Ref. [3].

4. Results for the Λ and Σ hyperons in nuclear matter

Recently, we investigated also the properties of our YN interactions in nuclear matter [4, 5]. Specifically, we performed conventional first-order Brueckner calculations based on the standard (gap) choice of the single-particle (s.p.) potentials [4] as well as with the continuous choice [5]. In the present work we focus on the results of Ref. [4].

The starting point of our nuclear matter calculation is the Bethe-Goldstone equation

$$\begin{aligned} \langle YN|G_{YN}(\zeta)|YN\rangle &= \langle YN|V|YN\rangle \\ &+ \sum_{Y'N} \langle YN|V|Y'N\rangle \, \langle Y'N|\frac{Q}{\zeta - H_0}|Y'N\rangle \, \langle Y'N|G_{YN}(\zeta)|YN\rangle \, , \end{aligned} \tag{2}$$

which defines the YN reaction matrix G_{YN}. Here, Q denotes the Pauli projection operator, which excludes those intermediate YN states with the nucleon inside the Fermi sea. The starting energy ζ in the Bethe-Goldstone equation (2) is defined by

$$\zeta = E_Y(p_Y) + E_N(p_N) \, , \tag{3}$$

where the single particle energies of the baryons are given by

$$E_\alpha(p_\alpha) = M_\alpha + \frac{p_\alpha^2}{2M_\alpha} + U_\alpha(p_\alpha), \qquad \alpha = Y,\ N, \tag{4}$$

i.e. these include the (nonrelativistic) kinetic energy and the baryon mass, and also the s.p. potential U_α. The nucleon s.p. potential U_N is taken from a separate calculation of pure nuclear matter based on a phenomenological NN potential, see the comment in Ref. [4], while the s.p. potential of the hyperons is calculated via

$$U_Y(p_Y) = \int_{p_N \le k_F} d^3p_N \, \langle YN|G_{YN}(\zeta(U_Y))|YN\rangle \, , \tag{5}$$

which means that it is determined self-consistently with Eq. (2) in the standard way. k_F is the Fermi momentum which is related to the nuclear matter density ρ via $\rho = (2/3\pi^2)\, k_F^3$. Finally, in lowest order in the so-called hole-line expansion [19], to which we restrict ourselves here, the binding energy of a hyperon in infinite nuclear matter is given by $B_Y(\infty) = -U_Y(p_Y = 0)$, evaluated at the saturation point of nuclear matter.

The strength of the s.p. spin-orbit potential of a hyperon in nuclear matter is most conveniently quantified by the so-called Scheerbaum factor S_Y [6], which is defined by [20]

$$U_\Lambda^{\ell s}(r) = -\frac{\pi}{2} S_Y \frac{1}{r}\frac{d\rho(r)}{dr} \boldsymbol{\ell}\cdot\boldsymbol{\sigma} \, . \tag{6}$$

Here $\rho(r)$ is the nucleon density distribution and ℓ the single-particle orbital angular momentum operator. The quantity S_Y can be expressed in terms of the (partial-wave projected) G-matrix elements in the form

$$\begin{aligned} S_Y(p_Y) &= -\frac{3\pi}{4(k_F)^3}\, \xi_Y(1+\xi_Y)^2 \sum_{I_0,J} \frac{2I_0+1}{(2I_Y+1)}(2J+1) \\ &\times \int_0^{p_{max}} \frac{d\,p}{(2\pi)^3}\, W(p,p_Y) \, \Big\{ (J+2)\, G^{J,I_0}_{Y1\,J+1,\,Y1\,J+1}(p,p;p_Y) \\ &+ G^{J,I_0}_{Y1J,Y1J}(p,p;p_Y) - (J-1)\, G^{J,I_0}_{Y1\,J-1,\,Y1\,J-1}(p,p;p_Y) \end{aligned}$$

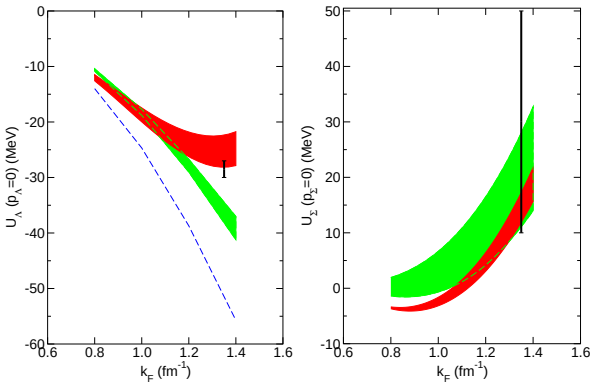

Fig. 2. The Λ and Σ s.p. potentials, $U_\Lambda(p_\Lambda = 0)$ and $U_\Sigma(p_\Sigma = 0)$, as a function of the Fermi momentum k_F. The green/grey band shows the chiral EFT results to LO for variations of the cut-off in the range Λ = 550–700 MeV, while the red/black band are results to NLO for Λ = 500–650 MeV. The dashed curve is the result of the Jülich '04 [18] meson-exchange potential. The vertical lines indicate the "empirical" range taken from Ref. [9].

$$- \sqrt{J(J+1)} \left[G^{J,I_0}_{Y1J,Y0J}(p,p;p_Y) + G^{J,I_0}_{Y0J,Y1J}(p,p;p_Y) \right] \Big\} \quad , \tag{7}$$

with $G^{J,I_0}_{YSL,Y'S'L'}$ being the matrix element for a specific total angular momentum J and isospin I_0 and outgoing and incoming spins (S, S') and orbital angular momenta (L, L'). The explicit expression for the weight function $W(p, p_Y)$ can be found in Ref. [4], together with a more detailed description of the formalism. ξ_Y denotes the mass ratio, $\xi_Y = M_N/M_Y$.

Let us now come to the results. Table I summarizes the values for the Λ and Σ potential depths, $U_\Lambda(p_\Lambda = 0)$ and $U_\Sigma(p_\Sigma = 0)$, evaluated at the saturation point of nuclear matter, i.e. for $k_F = 1.35$ fm^{-1}. Corresponding results obtained for the Jülich meson-exchange potentials from 2004 [18] and 1994 [21] are also included. In case of the EFT interactions we show the variation with the cutoff. These are comparable for U_Λ at LO and NLO, but noticeably reduced for U_Σ at NLO. The dependence of the hyperon potential depths on the Fermi momentum is displayed in Fig. 2.

The predictions for $U_\Lambda(0)$ at NLO for nuclear matter saturation density, as given in Table I, are well in line with the 'empirical' value for the Λ binding energy in nuclear matter of about −27 to −30 MeV, deduced from the binding energies of finite Λ hypernuclei [9].

Table I. Results for the s.p. potentials $U_\Lambda(0)$ and $U_\Sigma(0)$ (in MeV) and for the Scheerbaum factors S_Λ and S_Σ (in MeV fm^5) based on our EFT potentials and the Jülich meson-exchange interactions.

	EFT LO	EFT NLO	Jülich '04 [18]	Jülich '94 [21]
Λ [MeV]	550 · · · 700	500 · · · 650		
$U_\Lambda(0)$	−38.0 · · · −34.4	−28.2 · · · −22.4	−51.2	−29.8
$U_\Sigma(0)$	28.0 · · · 11.1	17.3 · · · 11.9	−22.2	−71.4
S_Λ	2.7 · · · 4.4	−3.7 · · · −3.7	−1.7	−0.4
S_Σ	8.4 · · · 13.1	−17.9 · · · −14.1	−13.3	−19.8

The predicted Σ s.p. potential is repulsive (at NLO and also at LO), see Table I. As already mentioned in the Introduction, this result is in agreement with evidence from the analysis of level

shifts and widths of Σ^- atoms and from measured (π^-, K^+) inclusive spectra related to Σ^--formation in heavy nuclei [22, 23]. We could achieve a repulsive Σ s. p. potential because the interaction in the $^3S_1$ partial wave of the $\Sigma^+ p$ channel (which provides the dominant contribution, cf. Table 4 in [4]) is repulsive, for the LO potential but also for the NLO interaction. Note, however, that with regard to the NLO interaction it had turned out that, in principle, the available YN scattering data can be fitted equally well with an attractive or a repulsive interaction in the $^3S_1$ partial wave of the isospin $I = 3/2$ ΣN channel [3]. The repulsive solution was adopted for the reasons just discussed, but also in accordance with results from a first lattice QCD calculation [24]. As exemplified by the predictions of the Jülich meson-exchange models, typically such phenomenological potentials fail to produce a repulsive Σ-nuclear potential.

Results for the Scheerbaum factor S_Λ that characterizes the strength of the Λ-nuclear spin-orbit potential in nuclear matter (cf. Eq. (6)) are also provided in Table I. While the results at LO are pure predictions, those at NLO depend on a LEC that generates $^1P_1$–$^3P_1$ transitions in the coupled ($I = 1/2$) ΛN–ΣN system, as already mentioned in the Introduction. This LEC has been set to zero in Ref. [3] because the YN data alone do not allow to establish a value for it. However, as shown in Ref. [4], it can be fixed by considering the Scheerbaum factor S_Λ calculated from the G-matrix, in conjunction with the constraint that the results for ΛN and ΣN scattering remain practically unchanged.

As guideline for the strength of the Λ-nucleus spin-orbit potential "empirical" values from studies of the splitting of the 5/2 and 3/2 states of ${}^{9}_{\Lambda}$Be by Hiyama et al. [25] and Fujiwara et al. [26] are used [4]. The results of those authors suggest that values for S_Λ in the order of -4.6 to -3.0 MeV fm^5 would be needed to reproduce the experimentally observed small level splitting. Values of around -3.2 and -4.1 MeV fm^5 are advocated in Refs. [27] and [28], respectively. Since the precise value required for the Λ s.p. spin-orbit strength can only be pinned down reliably via a dedicated calculation of finite hypernuclei based on our EFT interactions, we decided to aim at an exemplary result of -3.7 MeV fm^5. As one can see in Table I, this goal can be achieved.

5. Three-body forces

Besides an excellent description of the ΛN and ΣN data the chiral EFT interaction yields a satisfactory value for the hypertriton binding energy, see Ref. [3]. However, calculations for the four-body hypernuclei ${}^{4}_{\Lambda}$H and ${}^{4}_{\Lambda}$He based on the EFT interactions led to binding energies that are not consistent with the experimental results [29]. Specifically, the 0^+ state is considerably underbound by the NLO interaction. A similar underbinding is also observed for phenomenological models of the YN interaction [29]. Therefore, the question arises whether we see here the need for three-body forces. As already mentioned in the Introduction, in chiral EFT three-baryon forces (3BF) emerge automatically and can be derived consistently in this scheme. However, formally such 3BFs appear at next-to-next-to-leading order (NNLO) and, therefore, have not been included in the calculation presented in Ref. [29]. On the other hand, it is known from the three-nucleon sector that the three-nucleon forces (3NF) at NNLO are unnaturally large, which is connected with the excitation of the $\Delta(1232)$ resonance. Indeed, their effects are comparable to those one would expect at the NLO level. Moreover, in an EFT that includes the Δ isobar as explicit degree of freedom 3NFs appear already at NLO [1]. Thus, it is compelling to consider 3BFs already at the NLO level, specifically because in the ΛNN system the $\Sigma^*(1385)$ could play a similar role as the Δ for $3N$ [30, 31]. Note that in SU(3) chiral EFT that we apply all octet baryons (N, Λ, Σ, Ξ) are treated on equal footing. Accordingly, diagrams like $\Lambda NN \to \Sigma NN \to \Lambda NN$ mediated by two-meson exchange are reducible and do not constitute genuine three-baryon forces. Such diagrams are not part of the potential, but will be generated automatically when solving the Faddeev or Yakubovsky equations within a coupled-channel approach.

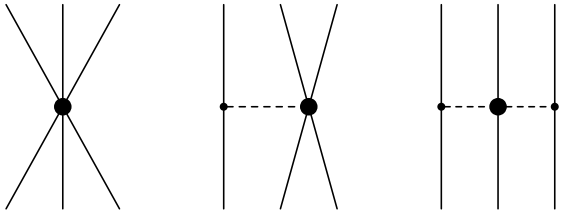

Fig. 3. Leading three-baryon interactions: contact term, one-meson exchange and two-meson exchange.

In Ref. [11] the leading 3BFs were derived within the framework of SU(3) chiral effective field theory, in complete analogy to the construction of the chiral nuclear forces [1]. Like in the $3N$ case at the order considered there are contributions from six baryon contact terms, from four-baryon contact vertex involving one pseudoscalar meson, and from two-meson exchange diagrams, see Fig. 3. In the following we sketch briefly the construction of the short-range contact contribution in SU(3) chiral EFT, corresponding to the diagram on the left hand side of Fig. 3. More details can be found in Ref. [11] where also the derivation of the other two contributions to the irreducible three-baryon potential at NNLO in the chiral power counting is presented.

The three-body force consists of the full set of the leading three-baryon contact interaction with a minimal number of low-energy constants, consistent with the symmetries of QCD. The construction of the chiral Lagrangian can be done analogously to the construction of the four-baryon contact terms. The symmetries of QCD have to be fulfilled namely charge conjugation, parity transformation, time reversal, Hermitian conjugation and (approximate) chiral symmetry. For the derivation of the potential it is also important to include the Pauli exclusion principle, since one starts with an overcomplete set of terms in the Lagrangian and wants to obtain the minimal number of low-energy constants. This can be achieved by an antisymmetrization in both the initial and the final state. The Pauli principle is not as restrictive as for the three-nucleon contact interaction, where one ends up with only one low-energy constant for the six-baryon contact term, but it is still relevant.

After constructing the pertinent terms in the chiral Lagrangian and performing a non-relativistic reduction, the leading potentials can be expressed through the following operators in spin space

$$1\,, \quad \vec{\sigma}_1 \cdot \vec{\sigma}_2\,, \quad \vec{\sigma}_1 \cdot \vec{\sigma}_3\,, \quad \vec{\sigma}_2 \cdot \vec{\sigma}_3\,, \quad \mathrm{i}\,\vec{\sigma}_1 \times \vec{\sigma}_2 \cdot \vec{\sigma}_3\,,$$

where the indices refer to the three initial baryons. For each three-baryon channel the prefactors of these spin operators are a combination of SU(3) coefficients and low-energy constants. A detailed analysis where all symmetry constraints are implemented leads to a total number of 18 independent low-energy constants for the three-baryon contact force [11]. As an explicit example let us provide the form of the potential for the ΛNN contact interaction. It is given by

$$\begin{aligned} V_{\mathrm{ct}}^{\Lambda NN} = \quad & C_1' \, (1 - \vec{\sigma}_2 \cdot \vec{\sigma}_3)(3 + \vec{\tau}_2 \cdot \vec{\tau}_3) \\ & + C_2' \, \vec{\sigma}_1 \cdot (\vec{\sigma}_2 + \vec{\sigma}_3) \, (1 - \vec{\tau}_2 \cdot \vec{\tau}_3) \\ & + C_3' \, (3 + \vec{\sigma}_2 \cdot \vec{\sigma}_3)(1 - \vec{\tau}_2 \cdot \vec{\tau}_3)\,. \end{aligned}$$

Here the Λ corresponds to the baryon with index 1, and the $\vec{\tau}$'s are the isospin operators of the two nucleons.

Note that the constant C_1' belongs exclusively to the transition with total isospin $I = 1$, whereas the constants C_2' and C_3' appear for total isospin $I = 0$. Interestingly, none of these three constants can be substituted by the constant E that appears in the corresponding three-body force of the purely nucleonic sector [1]. Thus, the strength of the ΛNN three-body contact interaction is not related to the one for NNN via SU(3) symmetry. As next step we intend to establish some estimates for the predominant low-energy constants. One possibility to achieve this goal is offered by the use of the

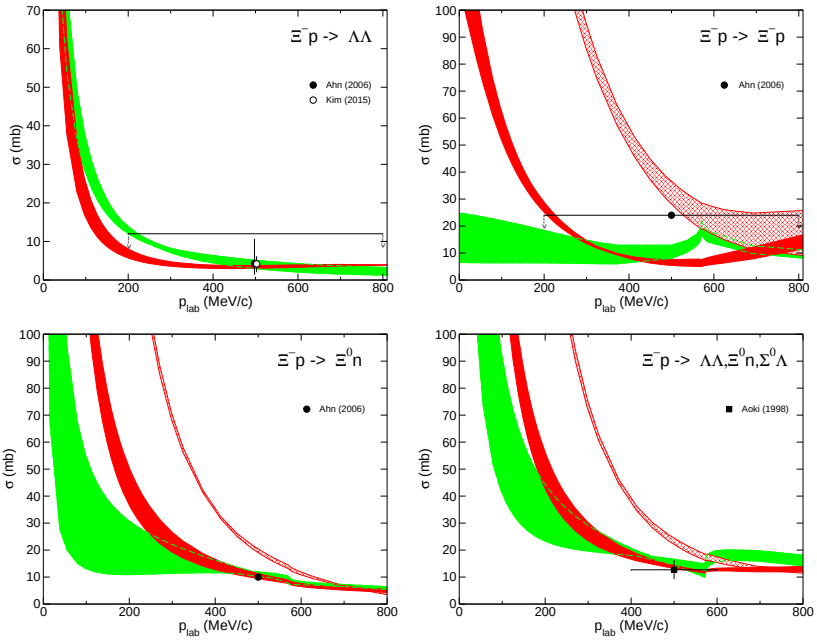

Fig. 4. $\Xi^- p$ induced cross sections. The bands represent our results at NLO (red/black) and LO (green/grey). The hatched band shows results based on $\tilde{C}^{8_a}_{^3S_1}$ from Ref. [3], see text. Experiments are from Ahn et al. [36] and Aoki et al. [37]. Upper limits are indicated by arrows.

so-called resonance saturation on the level of the decuplet baryons. For example, the Σ^* excitation can be used to evaluate part of the ΛNN two-pion exchange three-body interaction – just like the Δ in case of the NNN two-pion exchange three-body force.

6. Strangeness $S = -2$ sector

Results for baryon-baryon scattering in the strangeness $S = -2$ sector are presented in Fig. 4. Further results and a detailed description of the derivation of the interaction can be found in Refs. [12, 32].

In the application of chiral EFT to the $S = -1$ sector it had turned out that one can achieve a combined description of the ΛN and ΣN systems without any explicit SU(3) breaking in the contact interactions [3]. However, it also became clear that a simultaneous description of the YN data and the NN interaction, with contact terms fulfilling SU(3) symmetry strictly and consistently, is not possible. Specifically, the strength of the contact interaction corresponding to the 27-representation of SU(3) that is needed to reproduce the pp (or np) $^1S_0$ phase shifts is simply not compatible with the one required for the description of the empirical $\Sigma^+ p$ cross section [3, 33]. The same observation is now made in the extension to $S = -2$. If we simply take over all the low-energy constants as fixed from fitting to the ΛN and ΣN data then the $\Xi^- p$ cross sections turn out to be too large (hatched band) and the same happens for the $\Lambda\Lambda$ S-wave scattering length. Results that agree with the available measurements and upper bounds for the $\Lambda\Lambda$ and ΞN cross sections can be achieved, however, by re-adjusting some of the LECs, notably the leading S-wave contact terms corresponding to the 27 and 8_a irreducible SU(3) representations, $\tilde{C}^{27}_{^1S_0}$ and $\tilde{C}^{8_a}_{^3S_1}$ [12]. Results with readjusted LECs are shown as red/black bands in Fig. 4. We want to emphasize that an SU(3) breaking in the leading S-wave contact terms is in line with the employed power counting scheme [15]. Indeed, the LEC used in the 27 representation (in the $^1S_0$ partial wave) in the present calculation has been fixed by applying chiral

Table II. Scattering lengths (in fm) for $\Lambda\Lambda$, ΞN, and $\Sigma^+\Sigma^+$, for various cut-off values (in MeV).

		NLO				LO			
Λ		500	550	600	650	550	600	650	700
$\Lambda\Lambda$	a_{1S0}	−0.62	−0.61	−0.66	−0.70	−1.52	−1.52	−1.54	−1.67
$\Xi^0 p$	a_{1S0}	0.37	0.39	0.34	0.31	0.21	0.19	0.17	0.13
	a_{3S1}	−0.20	−0.04	0.021	0.039	0.02	0.00	0.02	0.03
$\Xi^0 n$	a_{3S1}	−0.25	−0.20	−0.26	−0.34	−0.34	−0.25	−0.20	−0.15
$\Sigma^+\Sigma^+$	a_{1S0}	−2.19	−1.94	−1.83	−1.82	−6.23	−7.76	−9.42	−9.27

EFT at NLO to the pp and $\Sigma^+ p$ systems with consistent inclusion of SU(3) breaking [33]. It has not been adjusted to $S = -2$ data.

Interestingly, the results based on our LO interaction from Ref. [32] (green/grey bands) are consistent with all empirical constraints. The cross sections at LO are basically genuine predictions that follow from SU(3) symmetry utilizing LECs fixed from a fit to the ΛN and ΣN data on the LO level.

S-wave scattering lengths for $\Lambda\Lambda$, ΞN, and $\Sigma^+\Sigma^+$, are compiled in Table II. The values for $\Xi^0 p$ and $\Xi^0 n$ are rather small and indicate that the ΞN interaction has to be relatively weak in order to be in accordance with the available empirical constraints. Indeed, the present results obtained in chiral EFT up to NLO imply that the published values and upper bounds for the $\Xi^- p$ elastic and inelastic cross sections [36, 37] practically rule out a somewhat stronger attractive ΞN force. The $\Lambda\Lambda$ $^1S_0$ scattering length is also fairly small. The value predicted by the NLO interaction is well within the range suggested by studies of the separation energy of the ${}^{\;\;6}_{\Lambda\Lambda}$He hypernucleus. It is also compatible with results for that scattering length obtained from analyses of the $\Lambda\Lambda$ invariant mass measured in the reaction $^{12}C(K^-, K^+\Lambda\Lambda X)$ [34] and of $\Lambda\Lambda$ correlations in relativistic heavy-ion collisions [35].

7. Summary

I presented selected results from the ongoing study of the baryon-baryon interaction within chiral effective field theory by the Jülich-Bonn-Munich Group. First, the in-medium properties of a hyperon-nucleon (YN) interaction derived within chiral EFT and fitted to ΛN and ΣN scattering data were discussed. The single-particle potentials for the Λ and Σ hyperons in nuclear matter were evaluated in a conventional G-matrix calculation, and the Scheerbaum factor associated with the Λ-nucleus spin-orbit interaction was computed.

The predictions for the Λ single-particle potential are found to be in good qualitative agreement with the empirical values inferred from hypernuclear data. A potential depth of about −25 MeV is predicted by the NLO YN interaction, and of about −36 MeV at LO. The Σ-nuclear potential turns out to be repulsive, in agreement with phenomenological information, with values around 15–20 MeV.

Empirical information suggests that the Λ-nucleus spin-orbit interaction should be rather weak. Therefore, we investigated also the spin-orbit interaction and, in particular, the role of a contact term that arises at NLO in the chiral expansion which provides an antisymmetric spin-orbit force in the YN system. It turned out that the strength of this contact term can be indeed fixed from investigating the properties of the Λ hyperon in nuclear matter and, specifically, it can be utilized to achieve a weak Λ-nuclear spin-orbit potential.

Recently the leading three-baryon forces have been derived consistently in SU(3) chiral EFT. The corresponding potentials which involve contact terms and irreducible one- and two-meson exchange diagrams were discussed. It is argued that the low-energy constants that arise in the three-body forces

of few-baryon systems with strangeness could be estimated by including decuplet baryons as explicit degrees of freedom.

Finally, results for the strangeness $S = -2$ sector suggest that the ΞN interaction has to be relatively weak in order to be in accordance with the available empirical constraints. In particular, the published data and upper bounds for the $\Xi^- p$ elastic and inelastic cross sections practically rule out a somewhat stronger attractive ΞN force. It should be mentioned, however, that the latest and still preliminary results from lattice QCD simulations apparently suggest a somewhat more attractive ΞN interaction [38].

Acknowledgements

I would like to thank N. Kaiser, U.-G. Meißner, A. Nogga, S. Petschauer, and W. Weise for collaborating on the topics covered by my talk. Work supported in part by DFG and NSFC (CRC 110).

References

[1] E. Epelbaum et al., Rev. Mod. Phys. **81** (2009) 1773.
[2] R. Machleidt and D. R. Entem, Phys. Rep. **503** (2011) 1.
[3] J. Haidenbauer *et al.*, Nucl. Phys. A **915** (2013) 24.
[4] J. Haidenbauer and U.-G. Meißner, Nucl. Phys. A **936** (2015) 29.
[5] S. Petschauer, J. Haidenbauer, N. Kaiser, U.-G. Meißner, and W. Weise, Eur.Phys.J. A **52** (2016) 15.
[6] R. R. Scheerbaum, Nucl. Phys. A **257** (1976) 77.
[7] E. Friedman and A. Gal, Phys. Rept. **452** (2007) 89.
[8] O. Hashimoto and H. Tamura, Prog. Part. Nucl. Phys. **57** (2006) 564.
[9] A. Gal, Prog. Theor. Phys. Suppl. **186** (2010) 270.
[10] E. Botta, T. Bressani, G. Garbarino, Eur. Phys. J. A **48** (2012) 41.
[11] S. Petschauer, N. Kaiser, J. Haidenbauer, U.-G. Meißner, and W. Weise, Phys.Rev. C **93** (2016) 014001.
[12] J. Haidenbauer, U.-G. Meißner, and S. Petschauer, arXiv:1511.05859 [nucl-th]; Nucl. Phys. A (2016), http://dx.doi.org/10.1016/j.nuclphysa.2016.01.006
[13] H. Polinder, J. Haidenbauer, and U.-G. Meißner, Nucl. Phys. A **779** (2006) 244
[14] J. Haidenbauer, U.-G. Meißner, A. Nogga, and H. Polinder, Lect. Notes Phys. **724** (2007) 113.
[15] S. Petschauer and N. Kaiser, Nucl. Phys. A **916** (2013) 1.
[16] C.M. Vincent and S.C. Phatak, Phys. Rev. C **10** (1974) 391.
[17] E. Epelbaum, W. Glöckle, and U.-G. Meißner, Nucl. Phys. A **747** (2005) 362.
[18] J. Haidenbauer and U.-G. Meißner, Phys. Rev. C **72** (2005) 044005.
[19] B.D. Day, Rev. Mod. Phys. **39** (1967) 719.
[20] Y. Fujiwara, M. Kohno, T. Fujita, C. Nakamoto, and Y. Suzuki, Nucl. Phys. A **674** (2000) 493.
[21] A. Reuber, K. Holinde, and J. Speth, Nucl. Phys. A **570** (1994) 543.
[22] M. Kohno, Y. Fujiwara, Y. Watanabe, K. Ogata, and M. Kawai, Phys. Rev. C **74** (2006) 064613.
[23] J. Dabrowski and J. Rozynek, Phys. Rev. C **78** (2008) 037601.
[24] S. R. Beane *et al.*, Phys. Rev. Lett. **109** (2012) 172001.
[25] E. Hiyama, M. Kamimura, T. Motoba, T. Yamada, and Y. Yamamoto, Phys. Rev. Lett. **85** (2000) 70.
[26] Y. Fujiwara, M. Kohno, K. Miyagawa, and Y. Suzuki, Phys. Rev. C **70** (2004) 047002.
[27] M. Kohno, Phys. Rev. C **81** (2010) 014003.
[28] Y. Fujiwara, M. Kohno, and Y. Suzuki, Mod. Phys. Lett. A **24** (2009) 1031.
[29] A. Nogga, Few Body Syst. **55** (2014) 757.
[30] R. Bhaduri, B. Loiseau, and Y. Nogami, Annals Phys. **44** (1967) 57.
[31] A. Gal, J. Soper, and R. Dalitz, Annals Phys. **63** (1971) 53.
[32] H. Polinder, J. Haidenbauer, and U.-G. Meißner, Phys. Lett. B **653** (2007) 29.
[33] J. Haidenbauer, U.-G. Meißner, and S. Petschauer, Eur. Phys. J. A **51** (2015) 17.
[34] A. M. Gasparyan, J. Haidenbauer, and C. Hanhart, Phys. Rev. C **85** (2012) 015204.
[35] K. Morita, T. Furumoto, and A. Ohnishi, Phys. Rev. C **91** (2015) 024916.
[36] J. K. Ahn *et al.*, Phys. Lett. B **633** (2006) 214.
[37] S. Aoki *et al.*, Nucl. Phys. A **644** (1998) 365.
[38] K. Sasaki *et al.*, arXiv:1504.01717 [hep-lat].